

An experimental investigation into the characteristics and performance of reactive powder concrete to choose the ideal mix

Azhar Ayad Jaafar ^{1,2*}, Alyaa Abdulrazzaq Azeez², Douread Raheem Hassen² and Mustafasanie M Yussof¹

¹School of Civil Engineering, Engineering Campus, Universiti Sains Malaysia, Nibong Tebal 14300, Pulau Pinang, Malaysia

²Ministry of Education, Najaf, Iraq

Abstract. reactive Powder Concrete (RPC) originated in the early 1990s as a cutting-edge concrete material renowned for its outstanding strength, durability, and ductility. Its remarkable durability attributes stem from a low water-cement ratio, high density, and elevated strength. With high ductility, RPC exhibits significant deformation capabilities before reaching failure. Additionally, its low porosity contributes to reduced material permeability, enhancing resistance against chemical attack and water infiltration. The primary goal of this experimental investigation is to choose an ideal mix for reactive powder concrete after implementing several experimental mixes based on mixing ratios implemented during previous studies to choose the optimal mix. Subsequently, the chosen mixture underwent testing at 7 days to assess its behavior and mechanical properties, utilizing six standard cylindrical specimens (10*20) cm and six cubes (15*15) cm. The results demonstrated a substantial increase in the ultimate compressive strength of the (RPC) specimen by 72% compared to the Normal Concrete (NC) specimen. Moreover, the tensile strength of the RPC exhibited a 35.4% increase compared to the (NC) specimen. The stress-strain analysis indicated a remarkable 118% increase in the (RPC) specimen's maximum stress compared to the (NC) counterpart. In contrast, the strain values for ordinary concrete rose by 22.5% at the point of maximum stress compared to the RPC specimen. Specifically, the tensile stress of the (RPC) specimen increased by 10% compared to the (NC), accompanied by a 29% uptick in tensile strain for the RPC specimen at the point of maximum stress. Furthermore, the (RPC) specimen demonstrated a 38.2% increase in the Modulus of Elasticity and a 35.7% increase in Poisson's ratio compared to the (NC) specimen.

1 Introduction

Over the past few years, there has been extensive application of advanced methods and materials in repairing, renovating, and strengthening reinforced concrete (RC) structures, primarily due to their exceptional performance characteristics. Despite numerous research efforts and studies dedicated to reactive powder concrete (RPC), there is currently no universally accepted design mix for RPC. Most RPC mixtures rely on experimental formulations and findings from prior studies. The RPC is an innovative form of concrete identified by the particles used diameter not surpassing (600 mm) and exceptionally elevated compression and tensile strength [1]. Many factors influence RPC efficiency, including fine silica fume ratio, steel fiber ratio, cementitious material, water-cement ratio, low porosity, and particle size typically less than 600 μm . Up to this point, developing a universally applicable design method has proven challenging [2]. The materials used in RPC exhibit outstanding performance attributes, featuring exceptional resistance capabilities that can achieve up to 200 MPa, along with elevated levels of toughness and ductility attributed to the inclusion of the steel fiber. These components contribute to improving the reactivity of RPC, leading to a new generation of cementitious materials characterized by outstanding mechanical properties arising from its densely packed microscopic structure [3]. The suggestion of using the integration of (SAW and Taguchi) methods was the most suitable approach for examining and optimizing RPC mix design [4]. Integrating a blend of macro and micro steel fibers at a proportion of 1.5% led to progressive improvements in the compressive strength, tensile strength, flexural strength, and flexural toughness of the specimens, increasing by 42.5%, 26.9%, 87.6%, and 39.6%, respectively [5]. The approach to microstructural alteration includes the removal of coarse particles and the integration of fine silica powders, along with micro-scale additives such as silica fumes (SF). The experimental findings indicated that RPC, with a water-to-binder ratio of 0.2, the inclusion of 2.5% superplasticizer, and curing with silica sand ranging from 150 to 600 μm in a water environment at 27°C, exhibited superior results concerning mechanical properties, composite characteristics, and practical as well as economic efficiency. It is noteworthy that while heat treatment notably enhances compressive strength,

* Corresponding author: azhar.farajallah@gmail.com

the combination demonstrates the overall optimal performance [6]. The enhanced compressive strength is probably associated with the introduction of the resonance input (V_f) within the tensile domain of RPC. This is corroborated by a confirmed comprehension of concrete's response to uniaxial compression, where failure is instigated by the lateral tensile stress resulting from the behavior of Poisson's ratio. Additionally, the characteristics of the RPC embedded in the (V_f) probe contribute to this phenomenon [7]. To achieve greater toughness, adding steel fibers can raise the cracking energy of RPC to a range between 20,000 and 40,000 J/m². Unlike standard concrete, RPC demonstrates tensile strength that is ten times higher and fracture energy that is two hundred times greater [8-10]. Furthermore, lowering the water-to-binder ratio leads to an ideal porous structure that is impermeable, thereby boosting the exceptional toughness of RPC [11, 12]. Due to its exceptional ductility, RPC offers enhanced structural precision through increased energy absorption [13]. Due to its elevated tensile strength, RPC can bear all significant tensile stresses within the same concrete, excluding tensile stresses. RPC is also distinguished by its exceptional resistance to abrasion, making it highly sought after in applications where physical wear is more common, such as bridge decks and industrial flooring [14]. Finally, the primary aim of this experimental investigation is to choose an ideal mix for reactive powder concrete after implementing several experimental mixes based on mixing ratios implemented during previous studies to choose the optimal mix.

2 Experimental program

The testing regimen comprises six cubes measuring (15 * 15 * 15) cm and six cylinders measuring (10 * 20) cm, all cast from (RPC) at the age of 7 days using three distinct mixtures. These specimens were then categorized into three groups for each sample type (cubes and cylinders). The appropriate mixture was chosen from among the three mixtures whose details are shown in Table 1. The curing of the specimens was conducted at both the 7-day and 28-day marks, followed by the execution of compression and tensile tests. Compression and tensile tests were conducted on the specimens utilizing a 2000-kilonewton capacity compression testing machine, as illustrated in Figure 1.

Table 1 Mixing ratios for trial mixtures

Groups	Cement Kg/m ³	Fine aggregate Kg/m ³	Silica fume *(%wc)	Super pl. *(%wc)	Steel fiber **(% All mix)	Water Kg/Litter	W/C
Group1	1000	1000	10	3	0.5	0.23	230
Group2	1000	1000	8	4	1	0.23	230
Group3	1000	1000	5	5	1.5	0.23	230

*(%wc) The quantity of silica fume expressed as a percentage of the cement weight.

**(%All mix) Amount of Steel fiber as a percentage of the weight of all mix.

2.1 Material specification

2.1.1 Cement

The casting of specimens (cubes and cylinders) employed locally available ordinary Portland cement from Najaf governorate, Iraq. Adheres to the Iraqi Standard Specification I.Q.S. No. 5 (IQS 1984) [15]. The authorized quantity of cement for the casting of (RPC) is 1000 kg/m³.

2.1.2 Fine Aggregate

This study made use of laboratory sand sourced locally from Najaf governorate, Iraq, as one of the components in the concrete mix. To achieve a highly compacted mixture of the RPC and fine sand aggregate an extremely fine gradation was utilized, excluding large particle sizes. The fine aggregate underwent a single classification process using a sieve with a maximum size of number 40 (450 μm) and an under the sieve of number 100 (150 μm) as per the method outlined by (Richard and Cheyreyzy 1995) [16]. The amount of fine sand adopted for casting the (RPC) is 1000 Kg/m³.

2.1.3 Silica Fume

An important characteristic of silica fume is its rapid and efficient blending capability, allowing for its application in specific small amounts to enhance the properties of concrete, as outlined in ACI 234R (ACI 1996) [17]. This study incorporated condensed silica fumes, specifically as a (Sika® Fume S 92 D). Micro-silica employed through this study conforms to the ASTM C1240 standards (ASTM 2015b) [18]. The amount of the silica fume, represented as a cement weight ratio, was (10%, 8%, and 5%).

2.1.4 Superplasticizer

GLENIUM® 54 is a contemporary advanced substance incorporated into concrete as a superplasticizer. These superplasticizers adhere to the standard specifications outlined by ASTM C494/C494M (ASTM 2015a) [19]. Typically, the superplasticizer is incorporated into the mix of the concrete as a ratio relative to the cement weight. Utilizing the proportions of (3%, 4%, and 5%) of the cement weight as a water-reducing admixture. When incorporated into a concrete mixture, this contemporary material possesses numerous attributes. It significantly decreases the necessary mixing water, improves workability, and enables the production of superior and (HSC) distinguished by increased porosity, thereby achieving optimal density.

2.1.5 Steel Fibers

The steel fibers serve as a replacement for coarse aggregate in the RPC mixture, imparting reinforcement properties and enhancing the ductility of the RPC. The steel fiber measures around 13 mm in length and has a diameter of approximately 0.2 mm, conforming to the specifications outlined in ASTM A820/A820M (ASTM 2011) [20]. The characteristics of the steel fibers are extracted from the manufacturer and detailed in Table 1. The quantities of steel fibers, expressed as a percentage of the total mixture weight, were (0.5%, 1%, and 1.5%).

Property	Value
Length	13 mm
Diameter	0.2mm
Density	7800kg/m ³
Tensile strength	2600 MPa
Aspect Ratio	65

Fig 1. Steel fiber characteristics

3 Specimens' preparation

In this investigation, cube molds and standard cylinders with dimensions (15*15) cm and (10*20) cm, respectively, were used to cast (RPC). The oil is applied in the mold to prevent concrete adhesion and facilitate easy removal of the mold. The combined materials were measured based on weight ratios specified for both ordinary concrete and RPC. A compact mixer has a capacity 0.25 cubic meters was utilized for blending the concrete components. Further information is depicted in Figures 2 and 3.



Fig 2. depicts the preparation of the materials mixing used in (RPC)



Fig 3. depicts the casting and specimens for the (RPC)

4 Designing the Concrete Mix

Before commencing the concrete mixing procedure, a slump Flow experiment was performed on the concrete mixture to verify adherence to the prescribed limits detailed in ASTM C 1611 [20], as illustrated in Figure 3. Various experimental combinations were tested through the investigation before arriving at the mixture necessary for RPC. All specimens (cubes, cylinders) had a ratio of 1:1 (cement: fine sand) with a water-to-cement ratio (W/C) of 0.23. Superplasticizer and silica fume were used at the rate of (3, 4, and 5) % and (10, 8, and 5) % by weight of the cement successively as well as the steel fibers, the percentage of the weight was (0.5, 1, and 1.5) % in all mixture details. Table 2 summarizes the compressive strength results for 7-day-old cube and cylinder specimens. The specifications and dimensions for casting specimens were determined according to the codes to ascertain the desired concrete properties:

- Cylinder with a height of 200 mm and a diameter of 100 mm following ASTM C39 [22]. for assessing compressive strength under ASTM C496 [23]. To evaluate the tensile strength, it will be used (The split-cylinder test).
- Cubes measuring with a dimensions 150 mm × 150 mm in accordance with ASTM C39 [22].



Fig 4. Slump test.

Table 2 Results of the specimens (Cubes & cylinders) for (RPC) after 7 days

Specimen symbol	*Average compressive strength ** f'_{cu} (MPa)			*Average compressive strength *** f'_{c} (MPa)		
	RPC	72.29	73.23	78.62	55.77	47.48
NC	17.5			14.8		

*Represents the average result of three specimens.

Considering the findings presented in Table 2, the mixing proportions of the initial group were selected to fulfill economic constraints (quantity reduction) while ensuring that there were no notable disparities in the achieved compressive strength results. The study revealed a reverse relationship between the quantities of silica fume and the amounts of superplasticizer and steel fibers. An increase in the amounts of silica fume led to higher compressive strength, while a decrease in the amounts of superplasticizer and steel fibers showed a similar trend.

Specimen symbol	* E_c (Exp.) (GPa)	* E_c (Eq.1) (GPa)	* E_c (Eq.2) (GPa)	* ν
NC	31.2	23.5	23.5	0.18
RPC	50.5	-----	-----	0.28

Fig 5. Properties related to the mechanics of the specimens

* E_c (EXP.) Concrete's modulus of elasticity in accordance with (ASTM C469-02) [25]. It computes it from the experimental outcomes for the stress-strain curve using the formula: slope = Rise/Run.

* E_c (Eq.1) Modulus of elasticity for regular concrete in accordance with (ACI-318M-14) [26] and determined using Equation 1. $E_c = 4700\sqrt{f'_{c'}}$

* E_c (Eq.2) Modulus of elasticity for standard concrete according to (ACI 363R-92) [27], calculated using Equation 2. $E_c = 3320\sqrt{f'_{c'}} + 6900$

* ν poison's ratio determined according to (ASTM C469-02) [25].

Note:

It's important to highlight that the two equations are specifically formulated to calculate (E_c) for conventional concrete, and currently, there is no existing equation for determining (E_c) for reactive powder concrete.

5 Testing Procedure

Once the curing process for the specimens was finalized at both the 7-day and 28-day intervals, they were extracted from the water. The specimens underwent testing utilizing a compression strength machine. Moreover, during the compression machine testing, precise properties, particularly the stress-strain curve, were obtained using a manually operated digital caliper and a mini digital thickness gauge, as shown in Figure 4.



Fig 6. The longitudinal and lateral strain gauge of concrete.

6 Findings and Analysis:

The experimental outcomes for specimens (cylindrical samples) aged 28 days are consolidated in Table 5. This includes data on ultimate compressive strength, ultimate tensile strength, concrete failure characteristics, and crack patterns. Additionally, an analysis and examination of the stress-strain curves for these specimens are presented and depicted in Figures 12-16.

During the compression test for normal concrete (NC), it was observed that the overall structure of the external concrete did not undergo significant damage, except for the emergence of vertical cracks resulting from compressive loading. This is attributed to the relatively weak resistance of ordinary concrete and its tendency to fail quickly, as depicted in Figure 5. The failure in the case of (NC) occurred when the compressive strength reached 22.5 MPa. The results indicate a sudden failure of the specimen, and the concrete failure behavior exhibited stability.

Conversely, during the splitting tensile test, it was observed that the (NC) underwent a tensile load and experienced failure with a fracture extending along the sample, dividing it into two equal parts. This can be attributed to the relatively weak tensile strength of ordinary concrete and the occurrence of sudden failure, as illustrated in Figure 6. The failure in (NC) transpired at a tensile strength of 4.52 MPa.

In the compression test for reactive powder concrete (RPC), it was noted that the upper portion of the sample was crushed, causing complete dislodgement of the external concrete without any cracking in the lower section of the sample. This outcome is attributed to the high strength of RPC and the presence of steel fibers that exhibit significant resistance to tensile forces, as depicted in Figure 7. The failure in RPC transpired when the compressive strength reached 80.3 MPa. The results indicate that the specimen took a considerable amount of time to fail, and the concrete's failure behavior was of the unstable type.

In contrast, during the splitting tensile test, it was observed that RPC underwent a tensile load, experiencing failure with multiple cracks extending along the sample. However, there was no separation of concrete parts due to the high tensile strength of RPC, which is enhanced by the presence of steel fibers that resist tensile forces and contribute to the concrete's hardness, as illustrated in Figure 8. Tensile failure in RPC occurred at a strength of 7 MPa.



Figure 7. concrete failure behavior under compression and crack pattern of (NC)



Figure 8. Concrete failure behavior under tensile and crack pattern of (NC)



Fig 9. concrete failure behavior under compression and crack pattern of (RPC)



Fig 10. concrete failure behavior under tensile and crack pattern of (RPC)

Specimen symbol	Ultimate compressive strength (MPa)	Ultimate tensile strength (MPa)	Increase in the compressive strength (%)	Increase in the tensile strength (%)
NC	22.5	4.52	0 (Reference)	0 (Reference)
RPC	80.3	7	72	35.4

Fig 11 . Experimental results of specimens

$$\% \text{ Increase} = \frac{F(\text{Reinforced}) - F(\text{Control})}{F(\text{Control})}$$

Applying ASTM C469-02 [25] to specimens of both (NC) and (RPC) yielded authentic data, subsequently represented in the curves of the stress strain. These curves illustrate the longitudinal and lateral stress-strain characteristics of the concrete compression zone for both (NC) and (RPC) specimens, as shown in Figures 12 and 13. A unified longitudinal stress-strain curve representing the concrete compression zone for both (NC) and (RPC) specimens was generated, along with an aggregate curve, enabling a comparison of results between these two specimens, as depicted in Figure 14.

Figure 14 exhibits the stress-strain curve of the reference (NC) specimen, revealing a decrease at the loading end. Conversely, the (RPC) specimen displays markedly different behavior, distinguished by higher stress and decreased strain. This is apparent from the higher peak and constrained extension of the curve in comparison to the (NC) specimen.

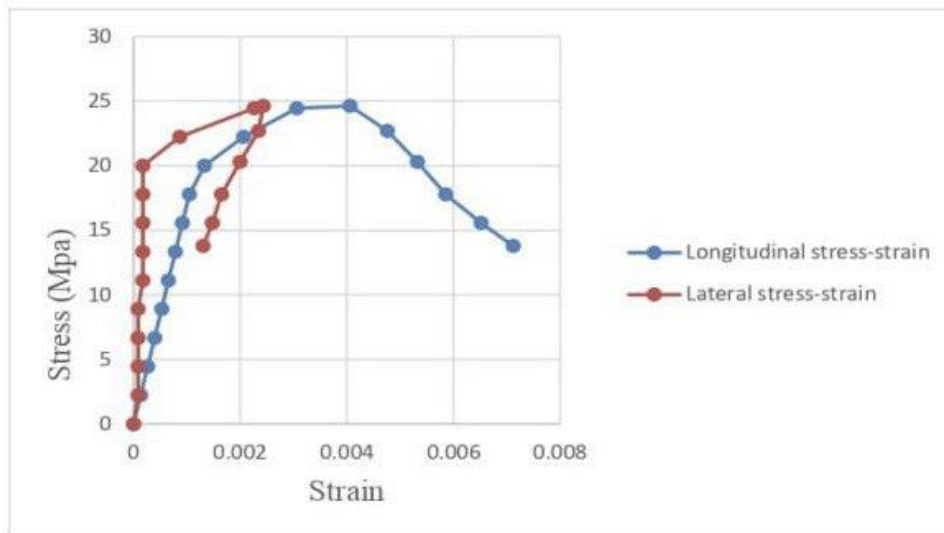


Fig 12. The stress-strain curve for the (NC) sample

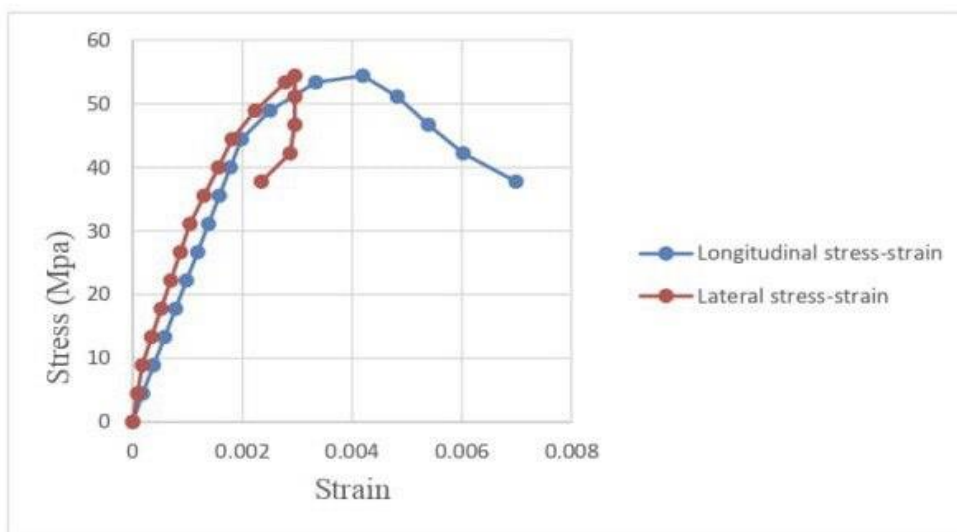


Figure 13. The stress-strain curve for the (RPC) sample

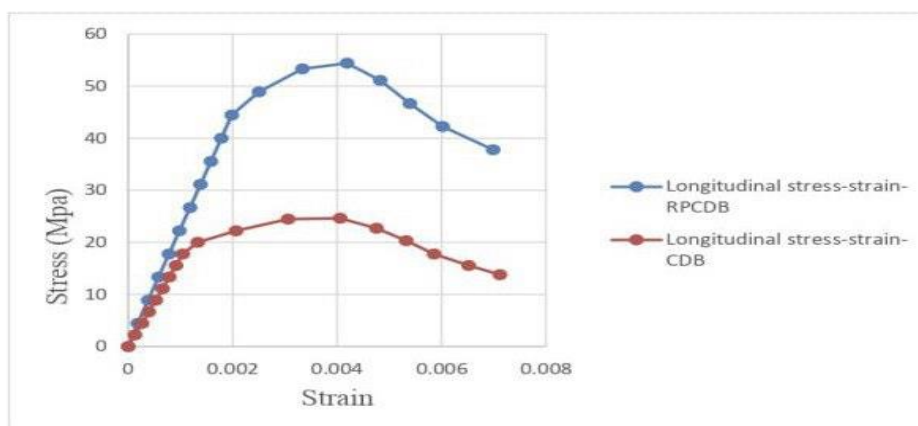


Figure 14. The stress-strain for (NC) & (RPC) specimens

The results of the stress-strain for the concrete tensile region in (NC) and (RPC) specimens were obtained through the split-cylinder test, adhering to the guidelines outlined in ASTM C496 [23]. Figure 15 illustrates these results.

Figure 15 displays stress-strain graphs depicting tension zone stress for both (NC) and (RPC) specimens. Notably, the (RPC) specimen exhibits higher tension stress and strain compared to the (NC) specimen. Specifically, the (RPC) specimen shows a 10% increase in tensile stress at maximum stress in comparison to the (NC) specimen. Moreover, the (RPC) specimen exhibits a 29% surge in tensile strain at maximum stress in contrast to the (NC) specimen.

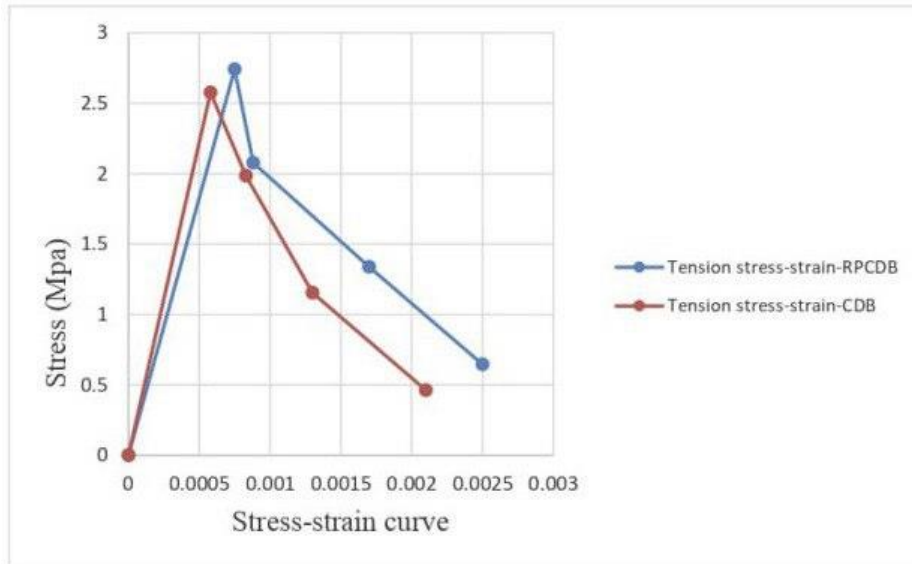


Fig 15. The stress-strain of the tension region in (NC) & (RPC)

All the results of stress-strain for samples (NC) & (RPC) were compared based on the results of previous studies as shown in Figure 16 and it showed an acceptable agreement with those results, which proves the validity of these laboratory results.

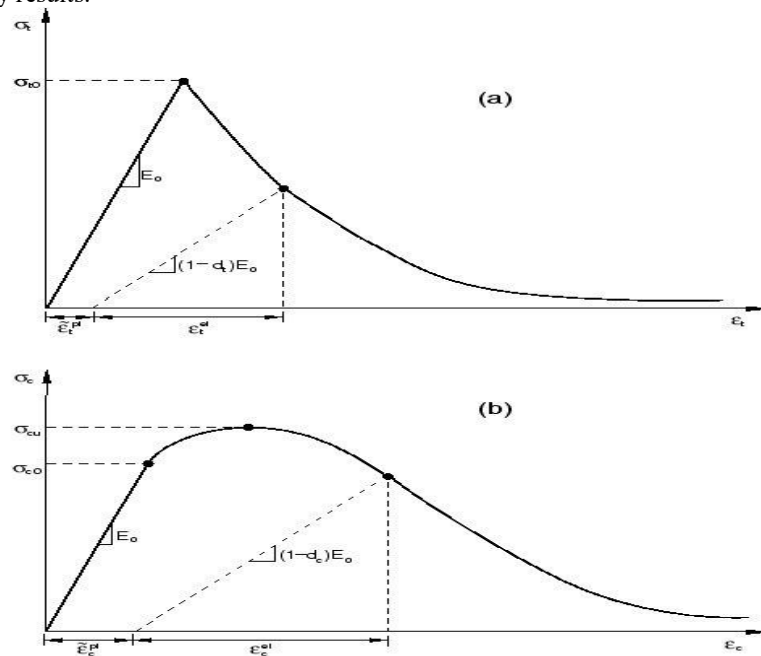


Fig 16. depicts stress-strain relationships for (a) the tension zone and (b) the compression zone in concrete

7 Conclusion:

After evaluating the outcomes of testing three experimental mixtures at a curing period of 7 days, the composition of the mixture was selected for Group No. (1). This mixture was deemed the optimal blend, meeting both economic constraints and providing the necessary strength. As a result, it was utilized in casting specimens at the age of 28 days.

Concerning the mechanical characteristics for the preferred blend in the (RPC) specimen, it exhibited a rise in both the Modulus of Elasticity and Poisson's ratio, with increases of (38.2% and 35.7%) respectively, in comparison to the (NC) specimen.

The incorporation of reactive powder concrete led to a notable exponential increase in the compressive strength of the (RPC) specimen. In this investigation, the ultimate compressive strength of the (RPC) specimen exhibited a significant rise of around 72% in comparison to the final compressive strength of the (NC) specimen.

The incorporation of reactive powder concrete resulted in a substantial exponential increase in the tensile strength of the (RPC) specimen. In this investigation, the ultimate tensile strength of the (RPC) specimen experienced an approximate 35.4% increase compared to the final tensile strength of the (NC) specimen.

The specimen results test, conducted following ASTM C469 [25] on both (NC) and (RPC), revealed that the stress outcomes of the (RPC) specimen exhibited a notable increase of (118%) at the ultimate stress in contrast to the (NC) specimen. In contrast, the strain measurements for the (NC) specimen indicated a rise of (22.5%) at maximum stress compared to the (RPC) specimen.

In the stress-strain outcomes acquired from the split-cylinder test following ASTM C496 [23], the (RPC) specimen demonstrated a (10%) augmentation in tensile stress at maximum stress in contrast to the (NC) specimen. Additionally, the (RPC) specimen displayed a (29%) surge in tensile strain at maximum stress relative to the (NC) specimen.

Reference

1. Chadli, M., Mekki, M., & Mezghiche, B. (2018). Formulation and study of metal fiber-reinforced reactive powder concrete. *World Journal of Engineering*, 15(4), 531-539]
2. Bae, B. I., Lee, M. S., Choi, C. S., Jung, H. S., & Choi, H. K. (2021). Evaluation of the ultimate strength of the ultra-high-performance fiber-reinforced concrete beams. *Applied Sciences*, 11(7), 2951]
3. Mostofinejad, D., Nikoo, M. R., & Hosseini, S. A. (2016). Determination of optimized mix design and curing conditions of reactive powder concrete (RPC). *Construction and Building Materials*, 123, 754-767]
4. Moslehi, A., Dashti Rahmatabadi, M. A., & Arman, H. (2023). Determination of Optimized Mix Design of Reactive Powder Concrete. *Advances in Civil Engineering*, 2023]
5. Mizani, J., Sadeghi, A. M., & Afshin, H. (2022). Experimental study on the effect of macro and microfibers on the mechanical properties of reactive powder concrete. *Structural Concrete*, 23(1), 240-254]
6. Tam, C. M., Tam, V. W., & Ng, K. M. (2010). Optimal conditions for producing reactive powder concrete. *Magazine of Concrete Research*, 62(10), 701-716]
7. Lee, N., & Chisholm, D. (2005). Reactive Powder Concrete, Study Report SR 146. *Ltd, Judgeford, New Zealand*]
8. Huynh, L., Foster, S., Valipour, H., & Randall, R. (2015). High strength and reactive powder concrete columns subjected to impact: Experimental investigation. *Construction and building materials*, 78, 153-171]
9. Liu, S., Xie, G., & Rao, M. (2013). Effect of waste glass powder on properties and microstructure of ultrahigh performance cement based materials. *Materials Research Innovations*, 17(sup1), 210-214]
10. Richard, P. (1996). A new ultra-high strength cementitious material. In *Proc. 4th Intl. Symp. on Utilization of High Strength/High Performance Concrete* (pp. 1343-1349)]
11. Matte, V., & Moranville, M. (1999). Durability of reactive powder composites: influence of silica fume on the leaching properties of very low water/binder pastes. *Cement and concrete composites*, 21(1), 1-9]
12. Yu, R., Spiesz, P., & Brouwers, H. J. H. (2014). Mix design and properties assessment of ultra-high performance fibre reinforced concrete (UHPFRC). *Cement and concrete research*, 56, 29-39]

13. Gao, R., Stroeven, P., & Hendriks, C. F. (2005). Mechanical properties of reactive powder concrete beams. *Special Publication*, 228, 1237-1252.]
14. Warnock, R. (2005). Short-Term and Time-Dependent Flexural Behavior of Steel-Fiber Reinforced Reactive Powder Concrete Beams. *University of New South Wales*.]
15. IQS (Iraqi Specifications of Central Agency for Standardization and Quality Control of Planning Council). 1984. Standard specification for portland cement. *IQS 5-1984. Baghdad, Iraq: IQS*.
16. Richard, P., & Cheyrezy, M. (1995). Composition of reactive powder concretes. *Cement and concrete research*, 25(7), 1501-1511.]
17. Aldred, J. M., Holland, T. C., Morgan, D. R., Roy, D. M., Bury, M. A., Hooton, R. D., ... & Jaber, T. M. (2006). Guide for the use of silica fume in concrete. *ACI-American Concrete Institute-Committee: Farmington Hills, MI, USA, 234*.]
18. ASTM. 2015b. Standard specification for silica fume used in cementitious mixtures. ASTM C1240. *West Conshohocken, PA: ASTM*.
19. ASTM. 2015a. Standard specification for chemical admixtures for concrete. ASTM C494/C494M. *West Conshohocken, PA: ASTM*.
20. ASTM, C. (2018). 1611-M14. Standard Test Method for Slump Flow of Self-Consolidating Concrete, 1, 1-6.]
21. ASTM Designation A615/A615M-01b, 2001, Standard Specifications for Deformed and Plain Billet-Steel Bars for Concrete Reinforcement, Annual Book of ASTM Standards, *American Society for Testing and Materials, Philadelphia, Pennsylvania, vol. 1.04*.
22. ASTM. 2018. Standard Test Method for Compressive Strength of Cylindrical Concrete Specimens. ASTM C39/C39M-18. *West Conshohocken, PA: ASTM*.
23. ASTM. 2017. Standard Test Method for Splitting Tensile Strength of Cylindrical Concrete Specimens. ASTM C496-96. *West Conshohocken, PA: ASTM*.
24. ASTM. 2018. Standard Test Method for Obtaining and Testing Drilled Cores and Sawed Beams of Concrete. ASTM C42/C42M-18a. *West Conshohocken, PA: ASTM*.
25. ASTM. 2002. Standard Test Method for Static Modulus of Elasticity and Poisson's Ratio of Concrete in Compression. ASTM C469-02. *West Conshohocken, PA: ASTM*.
26. ACI Committee 318, (2014). Building Code Requirements for Structural Concrete and Commentary. Reported by ACI Committee 318M, 2014.
27. ACI Committee-363, "State of the Art Report on High Strength Concrete (ACI 363R-92)," *American Concrete Institute, Detroit, 1997*.